ISSN 0021-3640, JETP Letters, 2017, Vol. 106, No. 6, pp. 384–389. © Pleiades Publishing, Inc., 2017.
Original Russian Text © V.Yu. Rudyak, M.N. Krakhalev, O.O. Prishchepa, V.S. Sutormin, A.V. Emelyanenko, V.Ya. Zyryanov, 2017, published in Pis'ma v Zhurnal Eksperimental'noi i Teoreticheskoi Fiziki, 2017, Vol. 106, No. 6, pp. 358–364.

CONDENSED MATTER

Orientational Structures in Nematic Droplets with Conical Boundary Conditions

V. Yu. Rudyak[a, *], M. N. Krakhalev[b, c], O. O. Prishchepa[b, c], V. S. Sutormin[b], A. V. Emelyanenko[a], and V. Ya. Zyryanov[b]

[a] *Faculty of Physics, Lomonosov Moscow State University, Moscow, 119991 Russia*
[b] *Kirensky Institute of Physics, Federal Research Center - Krasnoyarsk Scientific Center, Siberian Branch, Russian Academy of Sciences, Akademgorodok, Krasnoyarsk, 660036 Russia*
[c] *Institute of Engineering Physics and Radio Electronics, Siberian Federal University, Krasnoyarsk, 660041 Russia*
**e-mail: vurdizm@gmail.com*

Received July 24, 2017; in final form, August 24, 2017

Oblate nematic droplets encapsulated in a polymer specifying conical boundary conditions have been considered. Calculations by the extended Frank elastic continuum approach show that a number of various structures can be formed in such droplets under the variation of their size. Polarizing optical microscopy studies of composite film samples confirm the results of calculation and demonstrate the formation of the following orientational structures in the considered system: (i) a radial-bipolar structure with a twisted hedgehog defect and two hyperbolic boojums, (ii) an axial-bipolar structure with a circular disclination and two radial boojums, and (iii) a structure with a hedgehog defect, a hyperbolic boojum, and a radial boojum. Such a diversity of possible topologies of droplets is due to a complex balance between the energies of elasticity of the director field, disclinations, and anchoring with the surface, which is ensured by conical boundary conditions.

DOI: 10.1134/S0021364017180102

A liquid crystal composite material can be an ensemble of liquid crystal droplets surrounded by an isotropic medium [1–6]. The optical properties of such materials are determined primarily by the orientational structure, which is formed in liquid crystal droplets and can be easily controlled by external actions. In particular, the application of an electric field changes the orientational structure in liquid crystal droplets, which affects the optical properties of the entire material [7–10]. The configuration of the director in droplets can also be modified by light [11], by varying the temperature [12, 13], by the flow [14] or composition of a liquid surrounding liquid crystal droplets [15, 16].

The orientational structure of droplets depends on the properties of a liquid crystal material (elastic constant), geometry of the droplet (shape and size), boundary conditions (orientation of the director at the interface, anchoring energy), and an applied electric or magnetic field [9]. Spherical and ellipsoidal nematic droplets with tangential and homeotropic boundary conditions have already been well studied. In particular, bipolar [17], twisted bipolar [18], and toroidal [19] structures can be formed in droplets with tangential anchoring. A radial [17] or axial [20] configurations are formed in droplets under homeotropic boundary conditions. Droplets with conical boundary conditions where the angle between the director and the normal to the surface of the droplet is $0° < \theta_0 < 90°$ are less studied. In particular, in spherical droplets dispersed in a liquid matrix, a structure with two radial boojums and a circular defect can be formed and a structure with a radial boojum–hyperbolic boojum pair and a point defect in the bulk can be formed in a certain range of the director tilt angles θ_0 [12]. Conical anchoring conditions can appear, e.g., as intermediate between homeotropic and tangential conditions owing to an external action on the medium surrounding the liquid crystal droplet [16, 21–23]. In this case, the orientational structure varies smoothly from the radial to bipolar structure. The transformation of the structure is accompanied by change in the optical properties of droplets; for this reason, such systems can be used, e.g., to create highly sensitive sensors [24, 25].

In this work, we study the structure of oblate spheroidal liquid crystal droplets with conical boundary conditions. Such geometry of droplets is most often met in films of a polymer dispersed liquid crystal, which open wide prospects for application of composite liquid crystal materials. The structure of liquid crystal droplets is studied by computer simulation and polarizing optical microscopy.

The numerical simulation was performed within the extended Frank elastic continuum approach, where the energy of distortion of the director field, the energy of interaction of the liquid crystal with the surface, and the energy of disclinations are taken into account [26]. The director field was optimized by the Monte Carlo annealing method with the Metropolis criterion. The inclusion of the energy of interaction of the liquid crystal with the boundary of the droplet was adapted to the case of conical boundary conditions:

$$F = \int_V \left[\frac{K_{11}}{2} (\mathrm{div}\ \mathbf{n})^2 + \frac{K_{22}}{2} (\mathbf{n} \cdot \mathrm{rot}\ \mathbf{n})^2 + \frac{K_{33}}{2} [\mathbf{n} \times \mathrm{rot}\ \mathbf{n}]^2 \right] dV + \frac{W}{2} \int_\Omega [1 - \cos^2(\theta - \theta_0)] d\Omega + F_{\mathrm{def}},$$

where K_{11}, K_{22}, and K_{33} are the splay, twist, and bend elastic constants, $\mathbf{n}$ is the director field in the droplet, W is the anchoring energy per unit area, θ is the angle between the director and the normal to the surface, and θ_0 is the preferable tilt angle of the director.

The calculations were performed with the ratio $K_{11} : K_{22} : K_{33} = 1 : 0.5 : 1.3$ corresponding to the 5CB nematic liquid crystal [27] and the linear energy density of disclinations $f_{\mathrm{core}} = 10K_{11}$ [26]. The authors of [28, 29] showed that the most probable values for the anchoring energy W in homeotropically oriented nematic liquid crystal samples are 10^{-6}–10^{-5} J/m^2. The W values for planar-oriented nematic liquid crystals are larger, 10^{-5}–10^{-3} J/m^2. In our intermediate case, it is reasonable to perform calculations with the average value from the indicated range of 10^{-6}–10^{-3} J/m^2. It is convenient to use the dimensionless characteristic parameter WR/K_{11}, where $R = \sqrt[3]{R_x R_y R_z}$ is the reduced radius of the droplet and R_x, R_y, and R_z are the semiaxes of the spheroidal droplet.

For experimental studies of the orientational structures of nematic droplets with conical boundary conditions, we fabricated films of the polymer dispersed liquid crystal based on the poly(isobutyl methacrylate) (Sigma-Aldrich) and the LN-396 nematic mixture (Belarusian State Technological University) [30]. Composite film samples were fabricated by the TIPS phase separation technology [9] with the weight ratio of the components LN-396 : poly(isobutyl methacrylate) = 60 : 40. Because of the features of phase separation, liquid crystal droplets acquired the shape of an oblate spheroid with the short axis perpendicular to the film plane [9, 31]. The visible diameter of droplets in the plane of the sample d was in the range of 8–40 μm. Studies were performed with an Axio Imager.A1m polarizing optical microscope (Carl Zeiss) at a temperature of $t = 25$°C. The angle between the director and normal to the surface at the boundary of the droplet was $\theta_0 = 40° \pm 4°$.

The results of numerical simulation and experimental data demonstrate that several orientational structures characterized by different combinations and mutual arrangement of surface and bulk topological defects can be formed in oblate spheroidal droplets under conical boundary conditions.

As is known, a radial structure with a point hedgehog defect at the center of a droplet is observed in spherical [32] and oblate [26] droplets under homeotropic boundary conditions ($\theta_0 = 0°$) at a quite high energy of anchoring with the surface. In oblate droplets with the cone angle $\theta_0 = 40°$ in the case of a sufficient anchoring force at the boundary, a twisted radial-bipolar structure (**tRB**) with a point defect at the center of the droplet and two hyperbolic boojums located on the short axis of the spheroid can be observed (Fig. 1). The twisting of the structure at a nonzero cone angle makes it possible to prevent the formation of an additional linear defect on the surface of the droplet because it becomes energetically unfavorable at a strong surface anchoring. In view of symmetry, optical textures observed in a polarizing optical microscope do not change at the rotation of the sample with respect to polarizers (Figs. 1c–1e).

Structures with a pair of radial boojums and a circular surface disclination, the plane of which coincides with the center of the droplet (axial-bipolar structures), are formed at smaller dimensionless parameters WR/K_{11}. In this case, two variants of the orientation of the circular disclination on the surface are the most stable: (i) the disclination lies on the equator of the droplet (**AB**$_0$, Fig. 2) and (ii) the disclination is perpendicular to the equatorial plane of the droplet (**AB**$_{90}$, Fig. 3).

The bipolar axis in the **AB**$_0$ structure is close to the short axis of the spheroid (see Fig. 2b). For this reason, optical textures of the droplets hardly change at the rotation of the sample with respect to polarizers (see Figs. 2c–2e). The bipolar axis in the **AB**$_{90}$ structure coincides with the long axis of the droplet (see Fig. 3b). For this reason, optical textures strongly depend on the orientation of the bipolar axis of the structure with respect to polarizers (Figs. 3c–3e).

Two types of structures are observed at larger dimensionless parameters WR/K_{11}. The first structure (**sRB**) shown in Fig. 4 includes the radial and hyperbolic boojums, which are located at opposite points of the equatorial section of the droplet, and the bulk point defect located near the hyperbolic boojum.

The second structure (**sAB**) shown in Fig. 5 includes two radial boojums and a surface circular disclination significantly shifted toward one of the boojums. Such a structure is stabilized by a decrease in the length of the surface disclination, which compensates

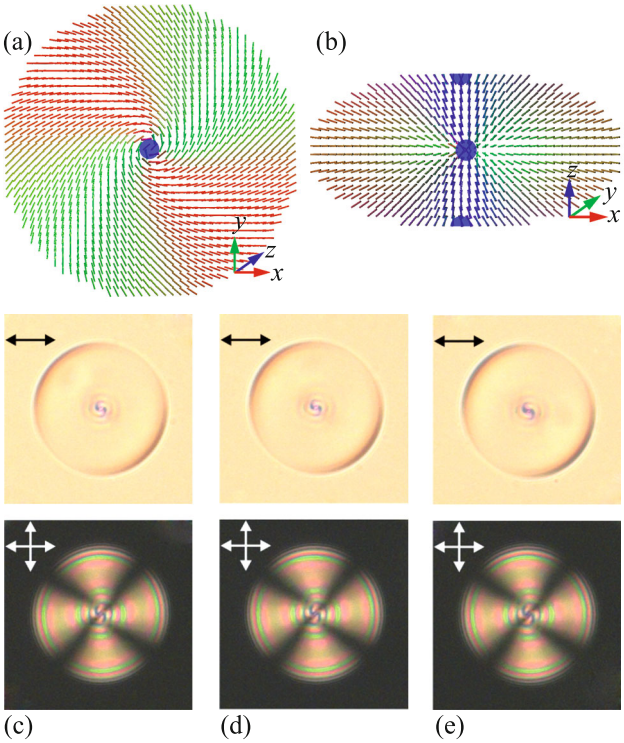

Fig. 1. (Color online) Twisted radial-bipolar structure with a point hedgehog defect at the center of a droplet and two hyperbolic boojums on the surface (**tRB**). Calculated configurations of the director in the plane passing through the center in the direction (a) normal to and (b) along the short axis of an oblate spheroid. The calculation was performed with the parameter $WR/K_{11} = 500$. (c–e) Photographs of the corresponding nematic droplet with a point defect at the center taken with the switched-off analyzer and crossed polarizers for the angles between the sample and polarizer of 0°, 45°, and 90°, respectively. The size of the droplet was $d = 24$ μm. Here and in other figures, red, green, and blue colors for the director field correspond to the directions with respect to the Ox, Oy, and Oz axes, respectively. Point defects in the bulk (hedgehogs) are marked by blue circles, whereas defects on the surface (boojums) are marked by semicircles. The orientations of polarizers are shown by double arrows.

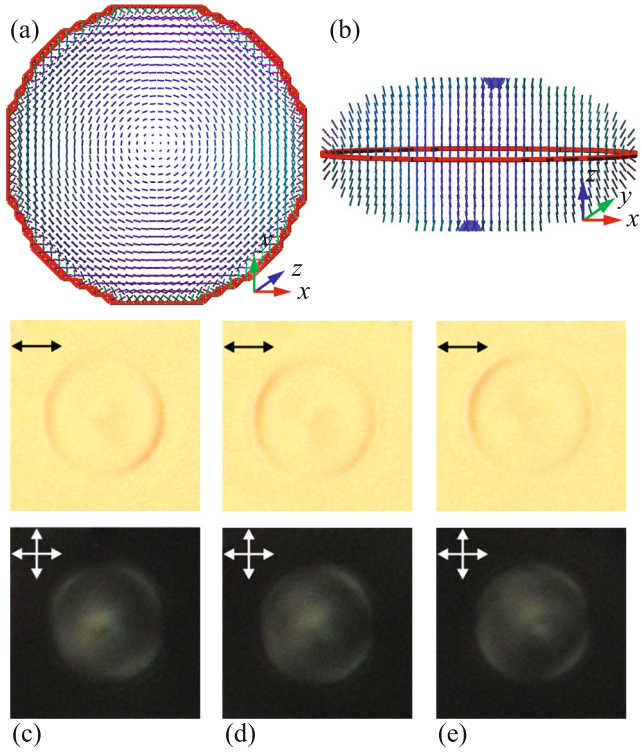

Fig. 2. (Color online) Axial-bipolar structure for the case where the surface circular disclination lies on the equator of the droplet (**AB**$_0$). Calculated configurations of the director in the plane passing through the center in the direction (a) normal to and (b) along the short axis of an oblate spheroid. The calculation was performed with the parameter $WR/K_{11} = 250$. Here and below, linear disclinations are shown by thick red lines. (c–e) Photographs of the corresponding nematic droplet taken with the switched-off analyzer and crossed polarizers for the angles between the sample and polarizer of 0°, 45°, and 90°, respectively. The size of the droplet was $d = 12$ μm.

the additional distortion of the director field. In both cases, since the bipolar axis of the structure lies in the plane of the polymer dispersed liquid crystal film, optical textures of droplets change noticeably at the rotation of the sample with respect to polarizers (see Figs. 4c–4e and Figs. 5c–5e).

In order to understand the origins of the formation of numerous different structures in the studied samples, we analyzed the relations between different energy contributions for all obtained variants of the structure of droplets. Figure 6 shows the contributions from surface anchoring, disclinations, and three types of elastic deformation to the total free energy of the system for the above configurations of droplets at $WR/K_{11} = 300$ (all energies are given in the dimensionless form, F_{total} is the total energy of the system, F_{sd} is the sum of the surface energy and the energy of surface disclinations, F_{el} is the energy of elastic deformations, F_{splay} is the splay energy, F_{twist} is the twist energy, F_{bend} is the bend energy). According to Fig. 6a, the **AB**$_0$, **sAB**, **tRB,** and **sRB** states have an almost identical free energy F_{total}, whereas the **AB**$_{90}$ state is insignificantly higher in energy. Thus, any of these states can occur in the samples at $WR/K_{11} = 300$. A change in the force of surface anchoring or in the size of the droplet will result in a change in the ratio WR/K_{11}. As a result, only some structures will become favorable because F_{sd} is proportional to WR/K_{11}, whereas changes in F_{el} will be insignificant and have a character of local adjustment. For example, axial-bipolar configurations **AB**$_0$ and **AB**$_{90}$ can be the most favorable at small ratios WR/K_{11}, whereas the **tRB** and **sRB** configurations are the most favorable at large

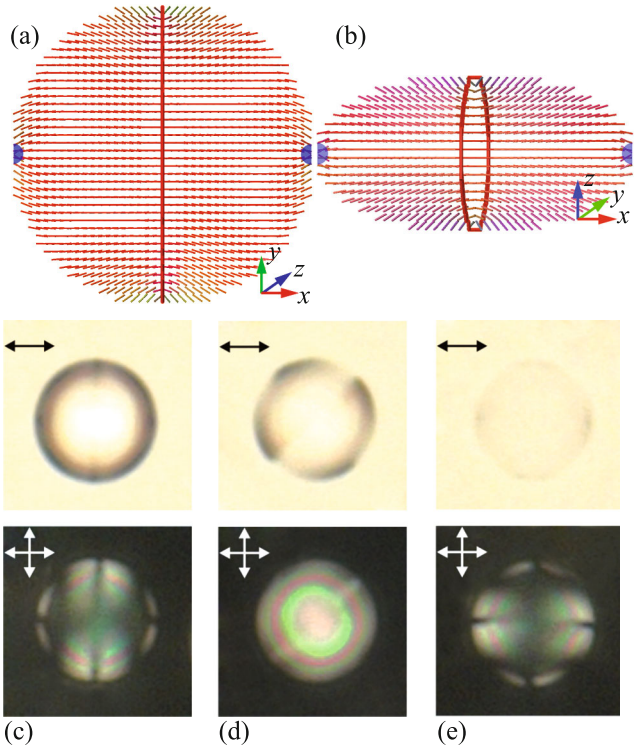

Fig. 3. (Color online) Axial-bipolar structure for the case where the surface circular disclination is perpendicular to the equator of the droplet (**AB**$_{90}$). Calculated configurations of the director in the plane passing through the center in the direction (a) normal to and (b) along the short axis of an oblate spheroid. The calculation was performed with the parameter $WR/K_{11} = 250$. (c–e) Photographs of the corresponding nematic droplet taken with the switched-off analyzer and crossed polarizers for the angles between the bipolar axis and polarizer of 0°, 45°, and 90°, respectively. The size of the droplet was $d = 12$ μm.

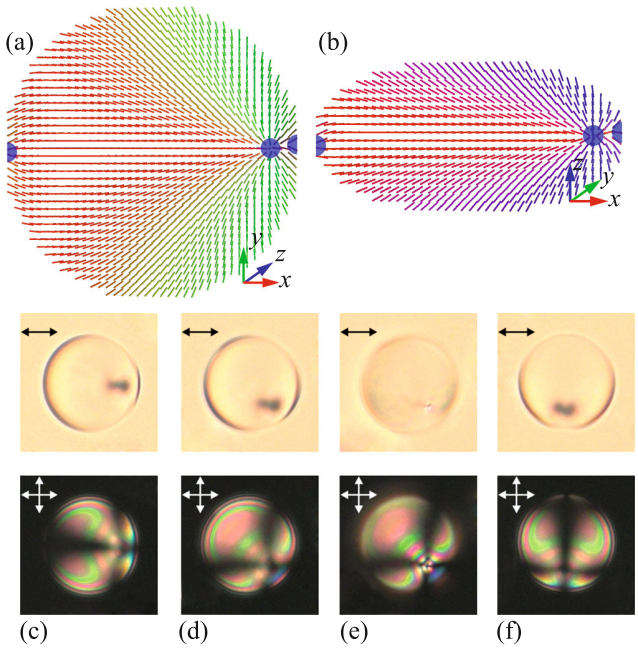

Fig. 4. (Color online) Structure with the hyperbolic and radial boojums and with the point defect in the bulk (**sRB**). Calculated configurations of the director in the plane passing through the center in the direction (a) normal to and (b) along the short axis of an oblate spheroid. The calculation was performed with the parameter $WR/K_{11} = 300$. (c–f) Photographs of the nematic droplet with a radial boojum and a "bulk point defect–hyperbolic boojum" pair taken with the switched-off analyzer and crossed polarizers when the angle between the projection of the bipolar axis and polarizer is (c) 0°, (d, e) 45°, and (f) 90°. The microscope was focused on the (e) bulk defect and (c, d, f) outer boundaries of the droplet. The size of the droplet was $d =$ 20 μm.

ratios WR/K_{11}. In experiments, this means that the probability of formation of a certain configuration depends on the size of droplets. In particular, some droplets smaller than 15 μm in the studied polymer dispersed liquid crystal films have only the axial-bipolar structure. Larger droplets include both the highly symmetric axial-bipolar structure and a configuration with a shifted circular disclination and the shift increases with the size of the droplets. Structures with point defects in the bulk of the droplet are observed in droplets larger than 20 μm.

An additional factor determining the stability of structures is the relation between elastic constants (see Fig. 6b). In particular, the structure with two hyperbolic boojums and a point defect at the center of the droplet (**tRB**) will prevail in nematic liquid crystals with a large elastic constant K_{11} (splay deformation), whereas the structure with the shifted bulk point defect (**sRB**) will be more favorable in nematic liquid crystals with a small elastic constant K_{11}.

To summarize, oblate spheroidal nematic droplets with conical boundary conditions have been studied theoretically and experimentally. It has been shown that the use of a simple Rapini surface potential with conical boundary conditions in the calculations of the director field gives significantly diverse possible structures in the considered droplets. When the angle between the director and the normal to the surface is $\theta_0 = 40°$, a number of configurations differing in type of topological defects and their mutual arrangement are formed in oblate droplets. The analysis of the contributions from the elastic and surface energies in different types of structures has showed that the studied structures become almost equivalent in free energy at the ratio of the product of the energy of anchoring with the surface and the radius of droplet to the elastic constant $WR/K_{11} = 300$. As a result, such structures can be simultaneously formed in a single sample, which is confirmed by experimental observations.

A structure with two hyperbolic boojums and a bulk point defect has been observed for the first time. The stability of the structure, as well as the absence of

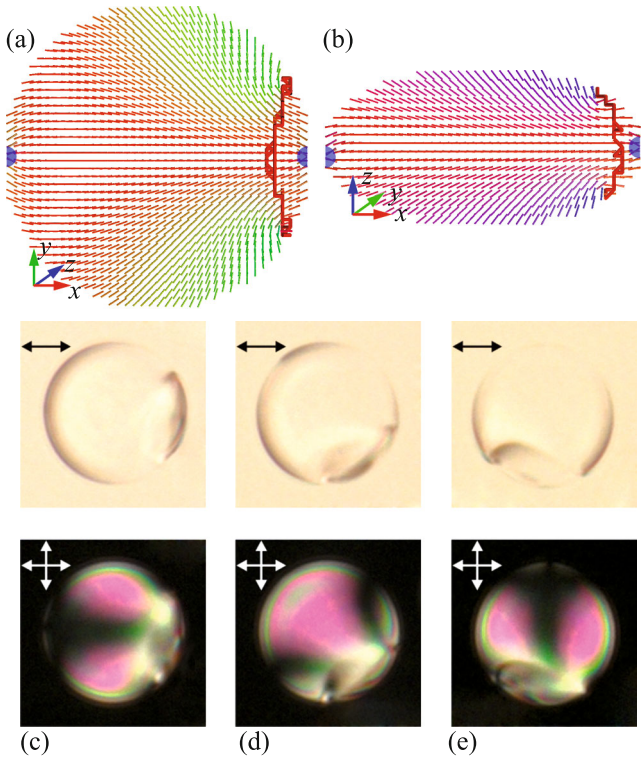

Fig. 5. (Color online) Structure with two radial boojums and a shifted circular defect (**sAB**). Calculated configurations of the director in the plane passing through the center in the direction (a) normal to and (b) along the short axis of an oblate spheroid. The calculation was performed with the parameter $WR/K_{11} = 300$. (c–e) Photographs of the nematic droplet with two boojums and the shifted circular defect taken with the switched-off analyzer and crossed polarizers for the angles between the bipolar axis and polarizer of 0°, 45°, and 90°, respectively. The size of the droplet was $d = 23$ μm.

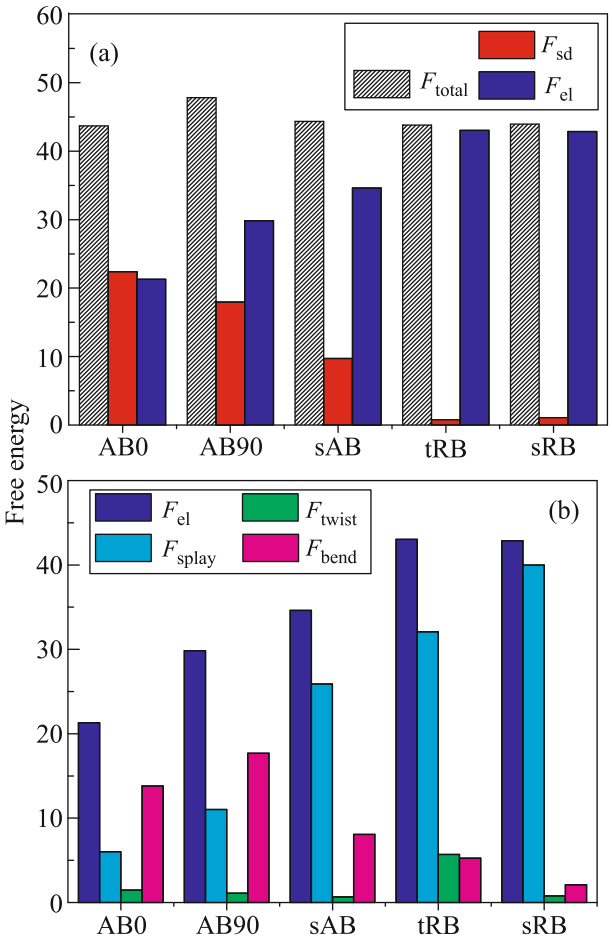

Fig. 6. (Color online) (a) Dimensionless free energy of the system F_{total} for various configurations and contributions of the energies of surface anchoring and surface disclinations (F_{sd}) and elastic deformations (F_{el}) at $\theta_0 = 40°$ and $WR/K_{11} = 300$. (b) Dimensionless energy of elastic deformations of various structures F_{el} and contributions of the splay F_{splay}, twist F_{twist}, and bend F_{bend} energies.

linear defects on the surface, is achieved by twist deformation in the bulk. The structure with a highly symmetric axial-bipolar configuration was previously observed in polymer dispersed liquid crystal films and emulsions [12, 30, 33, 34]. A low-symmetry structure with a radial boojum, a hyperbolic boojum, and a shifted point defect, as well as a structure with a pair of radial boojums and a shifted circular defect, was previously observed in emulsions of nematic droplets in the process of change in boundary conditions from normal to tangential and vice versa [12, 16, 21]. In this case, a change in the position of the bulk point or circular defect has been explained by a change in the angle between the director and the normal to the surface of the droplet. Our studies have revealed a more complex dependence of the positions of defects and the symmetry of the structure on the properties of the material including the size of the droplet, anchoring energy, and relation between the elastic constants of the nematic liquid crystal. The results obtained in this work can be used to design and develop functional materials and devices based on ensemble of nematic droplets, e.g., sensors.

This work was supported by the Russian Foundation for Basic Research and the Government of the Krasnoyarsk region (project no. 16-42-240704 r_a). The work of M.N. Krakhalev and V.S. Sutormin on the experimental study and analysis of the orientational structures of nematic droplets was supported by the Russian Foundation for Basic Research (project no. 16-32-00164). The work of V.Yu. Rudyak and A.V. Emelyanenko on the theoretical analysis of the structures of liquid crystal droplets was supported by the Russian Foundation for Basic Research (project nos. 15-02-08269 and 15-59-32410).

REFERENCES

1. M. Urbanski, C. G. Reyes, J. H. Noh, A. Sharma, Y. Geng, V. S. R. Jampani, and J. P. F. Lagerwall, J. Phys.: Condens. Matter **29**, 133003 (2017).
2. T. Lopez-Leon and A. Fernandez-Nieves, Colloid Polym. Sci. **289**, 345 (2011).
3. H.-S. Kitzerow and P. P. Crooker, Liq. Cryst. **16**, 1 (1994).
4. A. Darmon, M. Benzaquen, S. Copar, O. Dauchot, and T. Lopez-Leon, Soft Matter **12**, 9280 (2016).
5. L. Tran, M. O. Lavrentovich, D. A. Beller, N. Li, K. J. Stebe, and R. D. Kamien, Proc. Natl. Acad. Sci. **113**, 7106 (2016).
6. E. Pairam, J. Vallamkondu, V. Koning, B. C. van Zuiden, P. W. Ellis, M. A. Bates, V. Vitelli, and A. Fernandez-Nieves, Proc. Natl. Acad. Sci. **110**, 9295 (2013).
7. J. W. Doane, N. A. Vaz, B.-G. Wu, and S. Zumer, Appl. Phys. Lett. **48**, 269 (1986).
8. L. Bouteiller and P. le Barny, Liq. Cryst. **21**, 157 (1996).
9. P. S. Drzaic, *Liquid Crystal Dispersion* (World Scientific, Singapore, 1995).
10. S. A. Shvetsov, A. V. Emelyanenko, N. I. Boiko, J.-H. Liu, and A. R. Khokhlov, J. Chem. Phys. **146**, 211104 (2017).
11. J. Chen, E. Lacaze, E. Brasselet, S. R. Harutyunyan, N. Katsonis, and B. L. Feringa, J. Mater. Chem. C **2**, 8137 (2014).
12. G. E. Volovik and O. D. Lavrentovich, Sov. Phys. JETP **58**, 1159 (1983).
13. T. Orlova, S. J. Aßhoff, T. Yamaguchi, N. Katsonis, and E. Brasselet, Nat. Commun. **6**, 7603 (2015).
14. A. Fernandez-Nieves, D. R. Link, M. Marquez, and D. A. Weitz, Phys. Rev. Lett. **98**, 087801 (2007).
15. H. G. Lee, S. Munir, and S.-Y. Park, ACS Appl. Mater. Interfaces **8**, 26407 (2016).
16. J. K. Gupta, J. S. Zimmerman, J. J. de Pablo, F. Caruso, and N. L. Abbott, Langmuir **25**, 9016 (2009).
17. S. Candau, P. le Roy, and F. Debeauvais, Mol. Cryst. Liq. Cryst. **23**, 283 (1973).
18. P. S. Drzaic, Liq. Cryst. **26**, 623 (1999).
19. J. Jiang and D.-K. Yang, Liq. Cryst. (in press). doi 10.1080/02678292.2017.1301582
20. J. H. Erdmann, S. Zumer, and J. W. Doane, Phys. Rev. Lett. **64**, 1907 (1990).
21. D. S. Miller, X. Wang, and N. L. Abbott, Chem. Mater. **26**, 496 (2014).
22. A. V. Dubtsov, S. V. Pasechnik, D. V. Shmeliova, and S. Kralj, Appl. Phys. Lett. **105**, 151606 (2014).
23. A. V. Dubtsov, S. V. Pasechnik, D. V. Shmeliova, D. A. Semerenko, A. Iglic, and S. Kralj, Liq. Cryst. (in press). doi 10.1080/02678292.2017.1336676
24. M. Khan and S.-Y. Park, Colloids Surf. B: Biointerfaces **127**, 241 (2015).
25. U. Manna, Y. M. Zayas-Gonzalez, R. J. Carlton, F. Caruso, N. L. Abbott, and D. M. Lynn, Angew. Chem. Int. Ed. **52**, 14011 (2013).
26. V. Yu. Rudyak, A. V. Emelyanenko, and V. A. Loiko, Phys. Rev. E **88**, 052501 (2013).
27. G. P. Chen, H. Takezoe, and A. Fukuda, Liq. Cryst. **5**, 341 (1989).
28. L. M. Blinov, E. I. Kats, and A. A. Sonin, Sov. Phys. Usp. **30**, 604 (1987).
29. L. M. Blinov, A. Yu. Kabayenkov, and A. A. Sonin, Liq. Cryst. **5**, 645 (1989).
30. M. N. Krakhalev, O. O. Prishchepa, V. S. Sutormin, and V. Ya. Zyryanov, Liq. Cryst. **44**, 355 (2017).
31. O. O. Prishchepa, A. V. Shabanov, V. Ya. Zyryanov, A. M. Parshin, and I. G. Nazarov, JETP Lett. **84**, 607 (2006).
32. S. Kralj and S. Zumer, Phys. Rev. A **45**, 2461 (1992).
33. N. V. Madhusudana and K. R. Sumathy, Mol. Cryst. Liq. Cryst. **92**, 179 (1983).
34. Y.-K. Kim, S. V. Shiyanovskii, and O. D. Lavrentovich, J. Phys.: Condens. Matter **25**, 404202 (2013).

Translated by R. Tyapaev